J. Fluid Mech. (1995), *vol.* 290, *pp.* 203–212

Finite-amplitude three-dimensional instability of inviscid laminar boundary layers

By MELVIN E. STERN

Department of Oceanography, Florida State University, Tallahassee, FL 32306, USA

(Received 11 July 1994 and in revised form 7 December 1994)

An inviscid laminar boundary layer flow $\hat{U}(\hat{y})$ with vertical thickness λ_y, and free stream velocity U is disturbed at time $\hat{t} = 0$ by a normal velocity $\hat{v}$ and by a spanwise velocity $\hat{w}(\hat{x}, \hat{y}, \hat{z}, 0)$ of finite amplitude αU, with spanwise $(\hat{z})$ scale λ_z, and streamwise $(\hat{x})$ scale $\lambda_x = \lambda_z/\alpha$; the streamwise velocity $\hat{u}(\hat{x}, \hat{y}, \hat{z}, \hat{t})$ is initially undisturbed. A long wave $(\lambda_y/\lambda_z \to 0)$ expansion of the Euler equations for fixed α and time scale $\hat{t}_s = U^{-1}\lambda_z/\alpha$ results in a hyperbolic equation for Lagrangian displacements $\hat{y}$. Within the interval $\hat{t} > \hat{t}_s$ of asymptotic validity, finite parcel displacements $(O(\lambda_y))$ with finite $(O(U))$ $\hat{u}$ fluctuations occur, independent of α no matter how small; the basic flow $\hat{U}$ is therefore said to be unstable to streaky $(\lambda_x \gg \lambda_z)$ spanwise perturbations. The temporal development of the ('spot') region in the (x, z) plane wherein inflected $\hat{u}$ profiles appear is computed and qualitatively related to observations of 'breakdown' and transition to turbulence in the flow over a flat plate. The maximum $\hat{v}(\hat{x}, \hat{y}, \hat{z}, \hat{t})$ increases monotonically to infinity as $\hat{t} \to \hat{t}_s$.

1. Introduction

A key process in shear flow turbulence (Robinson 1991) is the development of spanwise circulations, since these produce the inflected streamwise velocity profiles within which relatively small-scale eddies are generated. In order to isolate this process many experiments have been done on the evolution of the laminar boundary layer in the flow over a flat plate in a wind tunnel. Although this non-inflected shear flow is stable to inviscid infinitesimal-amplitude perturbations, it is unstable to two-dimensional Tollmien–Schlichtung (TS) waves because of viscosity. Since these waves amplify very slowly, a vibrating ribbon in the upstream boundary layer has been employed to provide a finite initial amplitude, thereby reducing the downstream distance at which the TS waves are observed (Schubauer & Skramstad 1948). Subsequently (Klebanoff & Tidstrom 1958; Klebanoff, Tidstrom & Sargent 1961; Kovasznay, Komoda & Vasudevia 1962) a finite periodic spanwise modulation of the vibrating ribbon was use to produce controlled three-dimensional waves. The downstream phase speed and wavelength of these are consistent with linear TS theory, and the spanwise variation of growth rate is attributed (Klebanoff & Tidstrom 1959) to the variations in boundary layer thickness produced by the vibrating ribbon. The spanwise difference in amplitude increases downstream, giving rise to finite secondary circulations superimposed on the TS waves. Such spanwise motions can also develop naturally as a result of subharmonic or Floquet instability of finite-amplitude (two-dimensional) TS waves (Bayly, Orszag & Herbert 1988; Herbert 1988). Another possible mechanism (Bayly *et al.* 1988) involves the inviscid instability of an elliptical two-dimensional vortex, such as might be generated behind a trip wire placed at the leading edge of a plate (Hama, Long & Hegarty 1957).

The quasi-laminar three-dimensional phase ends and 'transition' begins when the spanwise circulation attains sufficient amplitude to produce an inflection in the streamwise velocity profile; this is correlated with low-velocity 'spikes' recorded by stationary velocity probes. Kovasznay *et al.* (1962) refer to the spike as an indicator of the initial 'breakdown' of the orderly flow, and refer to the region of the horizontal plane in which inflections occur as a 'spot'. The leading edge of this travels downstream with a speed slightly less than the free stream speed, and since the upstream end of the spot travels much slower, successive spots overtake each other in a region where the flow becomes 'turbulent'. Although the aforementioned evolution of the linear TS wave is interesting for its own sake, it may be possible to obtain a simpler starting point for understanding the transition stage, as suggested below.

Consider an inviscid laminar boundary layer flow in the $\hat{x}$-direction, with speed $\hat{U}(\hat{y})$ relative to the free stream speed U; so that $\hat{U}(0) = U$ is the speed at the wall ($\hat{y} = 0$), and $U(\hat{y}) = 0$ at $\lambda_y \leqslant \hat{y} < \infty$, where $\lambda_y = \hat{L}(\hat{x}, \hat{z}, 0)$ denotes the undisturbed height of an interface above which the flow is strictly irrotational. At time $\hat{t} = 0$ the flow beneath this interface is perturbated by a spanwise circulation whose $(\hat{z}, \hat{y})$ velocity components are $\hat{w}(\hat{x}, \hat{y}, \hat{z}, 0)$, $\hat{v}(\hat{x}, \hat{y}, \hat{z}, 0)$ respectively, and whose finite non-dimensional amplitude is defined by

$$\alpha \equiv -(U/\lambda_z)^{-1} \min \frac{\partial \hat{w}}{\partial \hat{z}}(\hat{x}, \hat{y}, \hat{z}, 0), \tag{1.1}$$

Let λ_z be the spanwise scale length of the disturbance, and let

$$\lambda_x = \lambda_z/\alpha \tag{1.2}$$

be the streamwise scale. A nonlinear long-wave solution of the three-dimensional Euler equations obtained (§2) by taking the limit

$$\lambda_y/\lambda_z \to 0 \tag{1.3}$$

for a fixed α leads to a hyperbolic differential equation (3.8) for the Lagrangian normal displacements. This equation depends on the basic shear flow ($\hat{U}$) (even though $\partial \hat{u}(\hat{x}, \hat{y}, \hat{z}, 0)/\partial \hat{x} = 0$), and is valid for $\hat{t} < \hat{t}_s = \lambda_z/\alpha U$, at which time the theory fails because the maximum normal velocity becomes infinite. But well before this time finite displacement $\hat{L} - \lambda_y = O(\lambda_y)$ occur which are independent of the initial amplitude (α) however small (but finite); likewise, finite streamwise fluctuations ($\hat{u}$) and finite inflections also develop. It is strongly suggested that the continuation of the calculation beyond $\hat{t}_s$, via the Navier–Stokes equations, will never lead to a return to the basic state, which is therefore said to be unstable.

The basic long-wave equation (3.2) has appeared previously (Stern & Paldor 1983, equation (57)) in another context, and also as the 'homobaric' approximation; see Russell & Landahl (1984) and references cited therein. The latter authors attempt to relate this approximation to transition in fully turbulent boundary layers by developing an (non-uniform) expansion of the Euler equations for small λ_y/λ_z and small $\hat{t} \ll \hat{t}_c$, where $\hat{t}_c$ is the estimated time at which the induced free stream pressure gradients generate non-negligible horizontal velocities. These pressures are computed from power series expansions in $\hat{t}$, and applied as a correction to the homobaric approximation. The resulting numerical calculations for $\lambda_y/\lambda_z = \frac{1}{5}$ exhibit inflections in the streamwise velocity profiles, but these occur at a time ($\hat{t} > \hat{t}_c$) beyond the limits of validity of the expansions.

The following development, on the other hand, is directed towards an understanding of the more restricted problem of the finite-amplitude instability of a laminar flow, and to the kind of transition mentioned in the previous experiments. The amplitude, length and time scalings in our long-wave ($\lambda_y/\lambda_z \to 0$) expansion are therefore chosen such as to make the pressure gradients negligible at all times within an interval ($\hat{t} < \hat{t}_s$) when streamwise inflections do appear. For small finite amplitudes (α) this manifestation of instability occurs for a spanwise scale (λ_z) much larger than Russell & Landahl's value ($\lambda_z = 5\lambda_y$), but still much smaller than the streamwise scale λ_x. This scale is in qualitative agreement with the observed 'streakiness' of the inflected spot, whose temporal evolution in the $(\hat{x}, \hat{z})$ plane (Figures 1–3) is also discussed.

Although the same kind of instability does not occur in the two-dimensional version ($\hat{w} \equiv 0$) of this problem, there is another noteworthy effect, viz. the temporal tendency for perturbed vorticity isopleths to concentrate in 'fronts'; i.e. large vorticity gradients form as a result of the homobaric tendency of fast moving parcels in the boundary layer to overtake slower ones. The experimental reality of this tendency was demonstrated (Stern & Vorapayev 1984) by discharging a dyed laminar (moderate Reynolds number) and axial symmetric jet from a round nozzle into a large tank of water. After a steady state (near the nozzle) was reached, the discharge was increased to a new steady value; during which time the fast fluid entering behind the slower jet formed a relatively broad transition region consisting of a weak downstream convergence. As time increased the fast fluid with relatively high (potential) vorticity overtook the slower fluid with lesser (potential) vorticity, thereby decreasing the width of the intervening transition zone, and forming a 'front' with large downstream vorticity gradient. This effect was accounted for by a cylindrically symmetric *long-wave* theory, using the same (homobaric) principle as is applied here in the context of a three-dimensional finite-amplitude instability.

The following theory extends the work of Ellingsen & Palm (1975), who showed that $\hat{U}(\hat{y})$ inflections can be forced by a pure spanwise ($\partial/\partial\hat{x} = 0$) and stationary finite-amplitude solution of the Euler equations; but unlike our case the $(\hat{v}, \hat{w})$ components are decoupled from the mean flow, and neither the boundary layer thickness (λ_y) nor the amplitude $\alpha \sim |\hat{w}|/U$ have any dynamical significance. The Ellingsen–Palm–Stuart mechanism is also central to viscous initial value calculations of the (linear) amplification of sub-critical and non-normal Orr–Sommerfeld modes (Butler & Farrell 1992; Trefethen *et al.* 1993). In the case of a boundary layer flow these studies show that optimal growth (before ultimate viscous decay) occurs for pure spanwise ($\partial/\partial\hat{x} = 0$) initial disturbances, whose normal velocity $\hat{v}$ produces the large changes in streamwise velocity which account for the increase in total disturbance energy. Some downstream variation must be present, however, for even the inclusion of finite amplitude will not alter the decay (Gustavsson 1991).

The possibility of 'bypassing' the two-dimensional Orr–Sommerfeld and secondary instability stages is raised by Henningson, Lundbladh & Johansson (1993), who first compute the linear viscous evolution of a specific (but nondescript) compact three-dimensional disturbance; this produces a temporally increasing long-wave component, in agreement with the aforementioned references. Then the initial amplitude is increased up to the point where inflected velocity profiles occur. A streamwise vortex then rolls up in this region, and small-scale turbulence ensues even though the Reynolds number is modest.

The result of the following inviscid theory, which includes nonlinearity and streamwise variation, suggests that the entire linear phase may be 'bypassed', in order to obtain a more direct route to the transitional phase.

2. Long-wave equations for the boundary layer

When the continuity and Eulerian momentum equations

$$\frac{\partial \hat{u}}{\partial \hat{x}}+\frac{\partial \hat{v}}{\partial \hat{y}}+\frac{\partial \hat{w}}{\partial \hat{z}}=0, \quad \left(\frac{\mathrm{d}\hat{u}}{\mathrm{d}\hat{t}}, \frac{\mathrm{d}\hat{v}}{\mathrm{d}\hat{t}}, \frac{\mathrm{d}\hat{w}}{\mathrm{d}\hat{t}}\right)=-\hat{\rho}^{-1}\left(\frac{\partial \hat{p}}{\partial \hat{x}}, \frac{\partial \hat{p}}{\partial \hat{y}}, \frac{\partial \hat{p}}{\partial \hat{z}}\right)$$

are made non-dimensional by the transformations

$$\left.\begin{aligned} \hat{z}=\lambda_z z, \quad \hat{y}=\lambda_y y, \quad \hat{x}=(\lambda_z/\alpha)\,x, \quad \hat{t}=(\lambda_z/\alpha)\,U^{-1}t, \\ \hat{u}=Uu(x,y,z,t), \quad \hat{w}=\alpha U w, \quad \hat{v}=\alpha U \epsilon v, \\ \hat{p}/\hat{\rho}=\epsilon\alpha^2 U^2 p(x,y,z,t), \quad \hat{L}=\lambda_y L(x,z,t), \quad \epsilon\equiv\lambda_y/\lambda_z. \end{aligned}\right\} \tag{2.1}$$

we get

$$\mathrm{d}u/\mathrm{d}t=-\epsilon\alpha^2\,\partial p/\partial x, \tag{2.2}$$

$$\mathrm{d}w/\mathrm{d}t=-\epsilon\,\partial p/\partial z, \tag{2.3}$$

$$\epsilon\,\mathrm{d}v/\mathrm{d}t=-\partial p/\partial y, \tag{2.4}$$

$$\partial u/\partial x+\partial v/\partial y+\partial w/\partial z=0. \tag{2.5}$$

Consider first an expansion of these equations in the boundary layer ($y<L$) for $\epsilon\to 0$ with α fixed. Then the leading-order terms in (2.2), (2.3), (2.5), are

$$\mathrm{d}u/\mathrm{d}t=0=\mathrm{d}w/\mathrm{d}t, \quad 0\leqslant y\leqslant L(x,z,t), \tag{2.6}$$

$$\partial u/\partial x+\partial v/\partial y+\partial w/\partial z=0, \tag{2.7}$$

and together with the boundary condition

$$v(x,0,z,t)=0 \tag{2.8}$$

constitute a complete set of initial value equations (cf. §3). But the value of the leading pressure term is not implicit in (2.4) because the constant of integration (in y) depends on the free stream ($y>L$) dynamics, and it is therefore important to verify the order of magnitude of p assumed in (2.1).

Note that the normal velocity

$$v(x,L,z,t)=\mathrm{d}L/\mathrm{d}t \tag{2.9}$$

computed from the (above) boundary layer dynamics will force horizontal velocities (u,w) in the irrotational free stream which are of the same order as (2.9), and all these fields (including p) vary relatively slowly in y, viz. on a ϵ^{-1} scale. Thus for the free stream region we set

$$y=\eta/\epsilon \tag{2.10}$$

in (2.2)–(2.5), and for the leading terms in the expansion of the fields we use

$$\left.\begin{aligned} u=\epsilon u_1(x,\epsilon y,z,t), \quad w=\epsilon w_1(x,\epsilon y,z,t), \\ v=v_1(x,\epsilon y,z,t), \quad p=p_1(x,\epsilon y,z,t). \end{aligned}\right\} \tag{2.11}$$

When $\epsilon\to 0$, (2.2)–(2.5) then reduce to

$$\frac{\partial u_1}{\partial t}=-\alpha^2\frac{\partial p_1}{\partial x}(x,\eta,z,t), \quad \frac{\partial w_1}{\partial t}=-\frac{\partial p_1}{\partial z}, \quad \frac{\partial v_1}{\partial t}=-\frac{\partial p}{\partial \eta}(x,\eta,z,t), \quad \frac{\partial u_1}{\partial x}+\frac{\partial v_1}{\partial \eta}+\frac{\partial w_1}{\partial z}=0, \tag{2.12}$$

since the nonlinear advective terms are higher in order in ϵ. At $\eta=\epsilon L\to 0$ the lower boundary condition for the solution of these linear equations becomes

$$v_1(x,0,z,t)=\partial L/\partial t \quad \text{at} \quad \eta=0. \tag{2.13}$$

This completes the first-order (in ϵ) asymptotics, which establishes that the effect of the horizontal pressure gradient in the boundary layer is indeed negligible for sufficiently small λ_y/λ_z, and at *all* t (and α) for which the solution of (2.6)–(2.8) is non-singular (finite). In addition the asymptotic value of the horizontal velocity on the interface is

$$u(x, L(x,z,t), z, t) = 0 = w(x, L(x,z,t), z, t). \tag{2.14}$$

3. Lagrangian dynamics

If $\bar{x}, \bar{y}, \bar{z}$ are the coordinates of a Lagrangian parcel at $t = 0$, and $x(\bar{x}, \bar{y}, \bar{z}, t)$, $y(\bar{x}, \bar{y}, \bar{z}, t)$, $z(\bar{x}, \bar{y}, \bar{z}, t)$ are its coordinates at t then the momentum equations (2.6) integrate to

$$x = \bar{x} + t\bar{u}(\bar{x}, \bar{y}, \bar{z}), \quad z = \bar{z} + t\bar{w}(x, \bar{y}, \bar{z}), \tag{3.1}$$

where $\bar{u}, \bar{w}$ are the given initial values of the horizontal velocity. It only remains to find the vertical position y of the parcel, and this is supplied by the Lagrangian continuity equation $\partial(x,y,z)/\partial(\bar{x},\bar{y},\bar{z}) = 1$. When (3.1) is used in the Jacobian determinant we get (Stern & Paldor 1983; Russell & Landahl 1984).

$$\begin{vmatrix} 1 + t\dfrac{\partial \bar{u}}{\partial \bar{x}} & \dfrac{\partial y}{\partial \bar{x}} & t\dfrac{\partial \bar{w}}{\partial \bar{x}} \\ t\dfrac{\partial \bar{u}}{\partial \bar{y}} & \dfrac{\partial y}{\partial \bar{y}} & t\dfrac{\partial \bar{w}}{\partial \bar{y}} \\ t\dfrac{\partial \bar{u}}{\partial \bar{z}} & \dfrac{\partial y}{\partial \bar{z}} & 1 + t\dfrac{\partial \bar{w}}{\partial \bar{z}} \end{vmatrix} = 1. \tag{3.2}$$

At any given t this inhomogeneous first-order equation can be integrated with respect to $\bar{y}$, starting with the boundary condition

$$y(\bar{x}, 0, \bar{z}, t) = 0, \tag{3.3}$$

to obtain the value of y for any $\bar{x}, \bar{y}, \bar{z}$. We emphasize the fact that these equations are independent of the amplitude (α) of the initial disturbance.

The solution will be discussed for the special, but most interesting, case in which the initial value of the streamwise velocity is the same as the undisturbed flow $\bar{u}(y)$, i.e.

$$u(x, y, z, 0) = \bar{u}(y), \quad \bar{u}(0) = 1, \quad u(1) = 0, \tag{3.4}$$

and the initial value of (w, v) is determined by

$$w(x, y, z, 0) = \bar{w}(\bar{x}, \bar{y}, \bar{z}) = \zeta(\bar{z})\,\phi(\bar{y})\,\Omega(\bar{x}), \tag{3.5}$$

where ζ, ϕ, Ω are given $O(1)$ functions. The normalization condition (1.1) and the non-dimensionalization in (2.1) require

$$\min \partial \bar{w}/\partial \bar{z} = -1, \tag{3.6}$$

and without further loss of generality we may take this minimum to occur at $\bar{z} = 0$, $\bar{x} = 0$, $\bar{y} = y_m$, so that

$$\zeta'(0) = -1, \quad \Omega(0) = 1, \quad \phi(y_m) = 1, \tag{3.7}$$

where the primes denote differentiation. Then (3.2) simplifies to

$$\begin{vmatrix} 1 & \partial y/\partial \bar{x} & t\zeta\phi\Omega'(\bar{x}) \\ t\bar{u}'(\bar{y}) & \partial y/\partial \bar{y} & t\zeta\phi'(\bar{y})\,\Omega \\ 0 & \partial y/\partial \bar{z} & 1 + t\zeta'(\bar{z})\,\phi\Omega \end{vmatrix} = 1. \tag{3.8}$$

It will be helpful if the names of the independent variables in this differential equation are now changed to (x_p, p, z_p), so that $(\bar{x}, \bar{y}, \bar{z})$ may be reserved for the initial values of the independent variables whose final values (x, y, z) are to be computed. With this understanding, (3.8) becomes

$$\frac{\partial y}{\partial p} - t\bar{u}'(p)\frac{\partial y}{\partial x_p} - \frac{t\zeta(z_p)[\Omega(x_p)\phi'(p) - \phi t\bar{u}'\Omega']}{1 + t\phi\zeta'\Omega}\frac{\partial y}{\partial z_p} = \frac{1}{1 + t\phi\zeta'\Omega}, \tag{3.9}$$

$$y(x_p, 0, z_p) = 0,$$

and we are required to compute y when $p = \bar{y}, x_p = \bar{x}, z_p = \bar{z}$.

The partial differential equation (3.9) is equivalent to the ordinary differential equation

$$\left[\frac{\mathrm{d}y}{\mathrm{d}p}(x_p(p), p, z_p(p))\right]_C = \frac{1}{1 + t\phi\zeta'\Omega}, \tag{3.10}$$

where differentiation is along the characteristic curve C obtained from

$$\frac{\mathrm{d}x_p}{\mathrm{d}p} = -t\bar{u}'(p), \quad x_p(\bar{y}) = \bar{x}, \tag{3.11}$$

$$\frac{\mathrm{d}z_p}{\mathrm{d}p} = \frac{-t\zeta[\Omega\phi' - t\phi\bar{u}'\Omega']}{1 + t\phi\zeta'\Omega}, \quad z_p(\bar{y}) = \bar{z}. \tag{3.12}$$

The integral of (3.11) yields a p-independent value of $x_p(p) + t\bar{u}(p)$, whose particular value at $p = \bar{y}$ equals x (3.1). Direct differentiation shows the solution of (3.12) is a p-independent value of $z_p(p) + t\zeta(z_p)\phi(p)\Omega(x_p)$, whose particular value at $p = \bar{y}$ equals z, (3.1). Thus the solutions

$$x_p(p) + t\bar{u}(p) = x, \tag{3.13}$$

$$z_p(p) + t\zeta(z_p)\phi(p)\Omega(x_p) = z, \tag{3.14}$$

determine C for any prescribed values of (x, z, t) and p. The geometrical interpretation of (3.13)–(3.14) is that all the Lagrangian points (at t) lying on a vertical line erected at x, z originated ($t = 0$) somewhere (i.e. at some p) on the characteristic curve obtainable by solving (3.13), (3.14) for x_p, z_p, Then the point on C with ordinate $p = \bar{y}$ ends up at an ordinate

$$y = \int_0^{\bar{y}} \frac{\mathrm{d}p}{1 + t\phi(p)\zeta'(z_p(p))\Omega(x_p(p))} \tag{3.15}$$

obtained by integrating (3.10) along the characteristic up to the point $p = y$. The vertical profile of streamwise velocity at (x, y, z, t) is then readily obtained from (2.6) and (3.4), which yield the conservation relation $u(x, y, z, t) = \bar{u}(y)$.

The solution becomes more explicit if $\bar{w}$ vanishes everywhere on the $z = 0$ plane, i.e.

$$\zeta(0) = 0, \quad \zeta'(0) = -1, \tag{3.16}$$

so that any Lagrangian point for which $\bar{z} = 0$ will have $z = 0$, and conversely. When (3.7) and (3.13) are used in (3.15), the result may be written as

$$y(\bar{x}, \bar{y}, 0, t) = \int_0^{\bar{y}} \frac{\mathrm{d}p}{1 - t\phi(p)\Omega(x - t\bar{u}(p))}, \tag{3.17}$$

where

$$\bar{x} = x - t\bar{u}(\bar{y}) \tag{3.18}$$

and

$$\bar{u}(\bar{y}) = u(x, y, z, 0) \tag{3.19}$$

is the basic flow which is independent of y, z. For any given $\bar{u}(\bar{y})$, and for any given components $\Omega(\bar{x})$, $\phi(\bar{y})$ of the initial spanwise velocity field ($\bar{w}$), we can integrate (3.17) at any (x, t) for a specified $\bar{y}$ to obtain the corresponding y. Then (3.19) gives the streamwise velocity at (x, y, t) and (3.18) gives its initial abscissa ($\bar{x}$).

The long-wave approximation to the z-component of vorticity

$$\omega = -\frac{\partial u}{\partial y}(x, y, 0, t) \tag{3.20}$$

can also be readily computed (Russell & Landahl 1984) by first differentiating (2.6) to get

$$\frac{\partial}{\partial z}\left(\frac{\partial}{\partial t}+u\frac{\partial}{\partial x}+v\frac{\partial}{\partial y}+w\frac{\partial}{\partial z}\right)w = 0, \tag{3.21a}$$

$$\frac{\partial}{\partial y}\left(\frac{\partial}{\partial t}+u\frac{\partial}{\partial x}+v\frac{\partial}{\partial y}+w\frac{\partial}{\partial z}\right)u = 0, \tag{3.21b}$$

When the derivatives are evaluated on $z = 0$ (where $w = 0$), the first of these equations becomes

$$\frac{\mathrm{d}}{\mathrm{d}t}\left(\frac{\partial w}{\partial z}\right)_0 = -\left(\frac{\partial w}{\partial z}\right)_0^2$$

or

$$\frac{\partial w}{\partial z}(x, y, 0, t) = \left(t+\left(\frac{\partial w}{\partial z}(x, y, 0, 0)\right)^{-1}\right)^{-1}. \tag{3.22}$$

With the help of the continuity equation (2.7), equation (3.21b) becomes

$$\frac{\mathrm{d}}{\mathrm{d}t}\left(\frac{\partial u}{\partial y}\right)_0 = \left(\frac{\partial w}{\partial z}\right)_0\left(\frac{\partial u}{\partial y}\right)_0,$$

and when (3.22) is used the result integrates to

$$\frac{\omega(x, y, 0, t)}{\omega(x, y, 0, 0)} = 1+t\frac{\partial w}{\partial z}(x, y, 0, 0) \tag{3.23}$$

$$= 1-t\phi(\bar{y})\,\Omega(\bar{x}). \tag{3.24}$$

If we follow the parcel at $\bar{x} = 0, \bar{y} = y_m$ with $\Omega(0) = 1$, $\phi(y_m) = 1$ we see that the vorticity vanishes at $t = t_s = 1$, and the long-wave theory fails at this point because the displacement y in (3.17) becomes infinite. Note that the normal velocity $v = (\partial y/\partial t)_{\bar{x}, \bar{y}}$ and the pressure gradient also become infinite.

The important generic point, however, as illustrated in the following section, is that for all $t < 1$ the Lagrangian parcel displacements $(y-\bar{y})$ and the horizontal velocity fluctuations $u(x, y, z, t)-\bar{u}(y)$ become $O(1)$, and independent of the value of the perturbation amplitude α.

4. Discussion and conclusions

Calculations for the quantities indicated above were made for

$$\bar{u}(\bar{y}) = (1-\bar{y})^2, \quad (\bar{y} \leqslant 1), \tag{4.1}$$

$$\Omega(\bar{x}) = 1/(1+(2\bar{x})^2), \tag{4.2}$$

$$\zeta(\bar{z}) = -\bar{z}/(1+(\bar{z})^2), \tag{4.3}$$

$$\phi(\bar{y}) = \begin{cases} \sin(4\pi\bar{y}) & \bar{y} < \frac{1}{2} \\ 0, & \bar{y} > \frac{1}{2}, \end{cases} \tag{4.4}$$

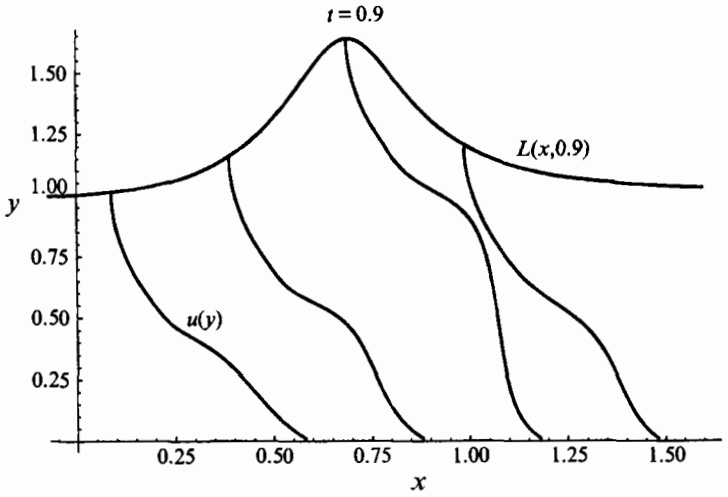

FIGURE 1. The vertical thickness $L(x, 0.9)$ of the boundary layer at $t = 0.9$, and four downstream velocity profiles ($u(y)$) on $z = 0$ for the initial conditions (4.1)–(4.4). The x-value which applies to each $u(y)$ profile is given by its intersection with $L(x, 0.9)$, and the velocity scale is given by $u(L) = 0$, $u(0) = 1$. Note that the displacement $L-1$ and the inflections are independent of the initial ($t = 0$) amplitude (α), and the homobaric theory is valid for $t < 1$.

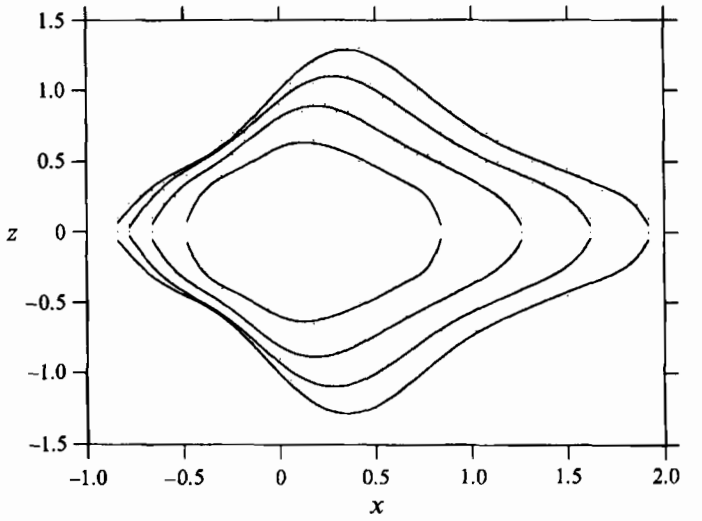

FIGURE 2. The area of the (x, z) plane within which an inflected u profile occurs. The initial conditions are the same as for figure 1, and the curves are for $t = 0.9$ (outermost), 0.7, 0.5 and 0.3. Note the difference in propagation rates of the leading and trailing edges of the 'spot'.

and

$$\phi(\bar{y}) = \begin{cases} \sin(2\pi\bar{y}) & \bar{y} < 1 \\ 0, & \bar{y} > 1 \end{cases}, \tag{4.5}$$

The spanwise velocity ($\hat{w}$) corresponding to (4.4) is horizontally convergent in $0 < \bar{y} < \frac{1}{4}$, and divergent for $\frac{1}{4} < \bar{y} < \frac{1}{2}$. Equation (3.17) applies on the $z = 0$ plane, and by setting $\bar{y} = 1$ the height $y = L(x, 0.9)$ of the vorticity interface (figure 1) on this plane was computed. The remaining curves ($u(y)$) in figure 1 are velocity profiles computed

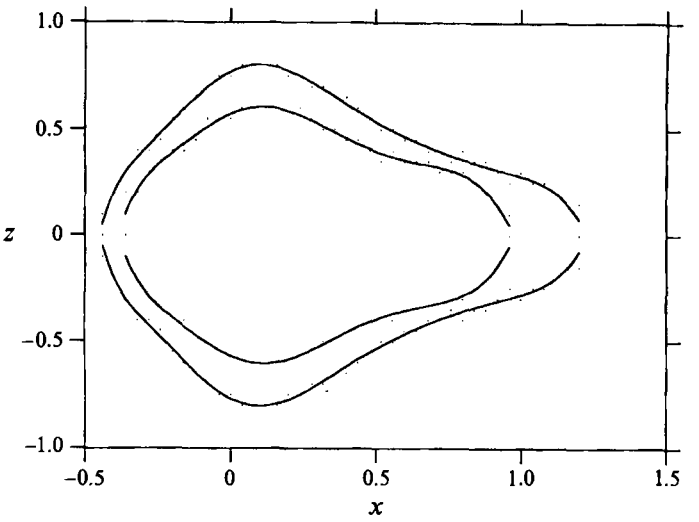

FIGURE 3. Same as figure 2 except that the initial disturbance (4.5) occupies the entire depth of the boundary layer. The curves ar for $t = 0.9$ and 0.7.

at the values of x where these curves intersect $L(x, 0.9)$, with $u = 0$ at these intersections, and $u = 1$ at $y = 0$. In a reference frame fixed to the wall, the free stream ($y > L$) would flow from right to left with unit speed, and at any fixed height the streamwise speed would be less than its undisturbed value. The region of minimum shear in u is explained (3.23) by the spanwise convergence and rising fluid in the lower boundary layer. The maximum vorticity (at $x = 0.7$) in the overlying inflection exceeds the maximum undisturbed value at $\bar{y} = 0$, because of the spanwise divergence of the rising fluid which originates at $\bar{y} > \frac{1}{4}$.

The more general integral (3.15) was use to compute the velocity profiles at x, z points for which $z \neq 0$. The area of the (x, z) plane within which an inflected u-profile may be found is indicated by the closed curves in figure 2 (for (4.4)) and figure 3 (for 4.5)). Figure 2 shows that the area of the 'spot' increases from zero at some time ($0 < t < 0.3$, not shown). Small-scale eddies may be expected to grow within the spot boundary, but the precise location of these curves in figures 2 and 3 is not significant; we may therefore say that the nose of the spot at negative x is almost stationary with respect to the free stream, while the nose of the spot at positive x is almost stationary with respect to the moving wall. Relative to the wall, the downstream ($x < 0$) end of the spot is moving faster than the upstream end, in qualitative agreement with the observation (cf. § 1) that one spot overtakes another at the downstream position where transition ends and turbulence begins. The theory also provides a qualitative explanation of the low-velocity 'spike' observed prior to this time. All of these finite effects are independent of the initial amplitude α, and only require larger values of dimensional time as α decreases. In the relevant regime of small α the theory 'predicts' a streaky ($\lambda_z < \lambda_x$) mode structure. This instability to small finite-amplitude disturbances is a generic property of our theory, which is associated with the fact that (3.17) $y - \bar{y}\, O(1)$ within the interval ($t < 1$) of validity of the long-wave theory. The total kinetic energy of the disturbance, as measured by the departure of $\hat{u}(\hat{x}, \hat{y}, \hat{z}, \hat{t})$ from its horizontal average (as well as by $\hat{w}, \hat{v}$), is much greater than its initial value, and $|\hat{v}| \to \infty$ as $t \to 1$.

The foregoing calculations could have been done for an initial disturbance which was periodic in x and z. It is interesting to speculate as to what would happen if our

inviscid solution at (say) $t = 0.5$ was used to initialize a numerical solution of the Navier–Stokes equations, in order to continue the calculation beyond the 'shock' points in space and time ($t = 1$), and to allow the small-scale eddies to grow in the inflected spot. Almost certainly the regime would not return to its undisturbed ($t = 0$) state, but 'new' spanwise motions would probably develop due to the dynamically significant horizontal pressure gradients which form when $t \to 1$. Some insight into what happens as $t \to 1$ may be obtained by comparing the long-wave theory for two-dimensional flow (Stern & Vorapayev 1984) with contour dynamical continuations for piecewise-uniform-vorticity shear flows (Stern 1989).

REFERENCES

BAYLY, J. B., ORSZAG, S. A. & HERBERT, T. 1988 Instability mechanisms in shear flow transition. *Ann. Rev. Fluid Mech.* **20**, 359–391.

BUTLER, K. M. & FARRELL, B. F. 1992 Three-dimensional optimal perturbations in viscous shear flow. *Phys. Fluids* A **4**, 1637–1649.

ELLINGSEN, T. & PALM, E. 1975 Stability of linear flow. *Phys. Fluids* **18**, 487–488.

GUSTAVSSON, L. H. 1991 Energy growth of three-dimensional perturbations in plane Poiseville Flow. *J. Fluid Mech.* **224**, 241–260.

HAMA, F. R., LONG, J. D. & HEGARTY, J. C. 1957 On transition from laminar to turbulent flow. *J. Appl. Phys.* **28**, 388–394.

HENNINGSON, D. S., LUNDBLADH, A. & JOHANSSON, A. V. 1993 A mechanism for bypass transition from localized disturbances in wall bounded shear flows. *J. Fluid Mech.* **250**, 169–207.

HERBERT, T. 1988 Secondary instability of boundary layers. *Ann. Rev. Fluid Mech.* **20**, 487–526.

KLEBANOFF, P. S. & TIDSTROM, K. D. 1959 Evolution of amplified waves leading to transition in a boundary layer with zero pressure gradient. *NASA Tech Note* D195.

KLEBANOFF, P. S., TIDSTROM, K. D. & SARGENT, L. M. 1962 The three dimensional nature of boundary layer instability. *J. Fluid Mech.* **12**, 1–34.

KOVASZNAY, L. S. G., KOMODA, H. & VASUDEVIA, R. B. 1962 Detailed flow field in transition. In *Proc. 1962 Heat Transfer and Fluid Mechanics Institute of University of Washington*, pp. 1–26.

ROBINSON, S. T. 1991 Coherent motions in turbulent boundary layers. *Ann. Rev. Fluid Mech.* **23**, 601–639.

RUSSELL, J. M. & LANDAHL, M. T. 1984 The evolution of an eddy near a wall in an inviscid shear flow. *Phys. Fluids* **27**, 557–570.

SCHUBAUER, G. B. & SKRAMSTAD, H. K. 1948 Laminar boundary layer oscillations and transition on a flat plate. *Natl Advis. Comm. Aeron. Tech. Rep.* 909.

STERN, M. E. 1989 Evolution of locally unstable shear flow near a wall or a coast. *J. Fluid Mech.* **198**, 79–99.

STERN, M. E. & PALDOR, N. 1983 Large amplitude waves in a shear flow. *Phys. Fluids* **26**, 906–919.

STERN, M. E. & VORAPAYEV, S. J. 1984 Formation of vorticity fronts in shear flow. *Phys. Fluids* **4**, 848–854.

TREFETHEN, L. N., TREFETHEN, A. E., REDDY, S. C. & DRISCOLL, T. A. 1993 Hydrodynamic stability without Eigen values. *Science* **261**, 578–584.